



Rare earth element oxides for tracing sediment movement

V.O. Polyakov*, M.A. Nearing

Ohio State University, 422D Kottman Hall, 2021 Coffey Road, Columbus, OH 43210, USA

Southwest Watershed Research Center, 2000 East Allen Road, Tucson, AZ 85719, USA

Received 1 November 2002; received in revised form 1 April 2003; accepted 3 June 2003

Abstract

The development of soil conservation plans and evaluation of spatially distributed erosion models require knowledge of rates of soil loss and sedimentation on different landscape elements and slope positions. Characterization of soil erosion rates and patterns within watersheds is important for the understanding of erosion processes and landscape evolution. Experimental data that show spatial translocation of soil on slopes are limited. A method for obtaining spatially distributed information on sediment movement employing rare earth element (REE) oxides is proposed. Five REE oxides in powder form were uniformly mixed with the soil on different parts of a 10% slope in a 4×4 m soil bed. Particle translocation was measured during eight simulated rainfalls at 60 mm h⁻¹ intensity. A laser scanner was utilized to obtain digital elevation models (DEMs) of the soil surface that were used as the reference data to compare with the tracer method. REE concentration in soil and runoff samples was determined by inductively coupled plasma mass spectrometry (ICP-MS). Erosion rates for different slope positions estimated from REE concentrations correlated with those calculated from the DEMs with relative differences for different slope sections of 4–40%. The enrichment ratio for this type of tracer was 1.7. The amount of sediment produced on different parts of the slope varied, with the greatest erosion occurring on the upper-middle part of the slope. The experiment showed that the multi-element tracer method provided a satisfactory way to study soil erosion distribution on a uniform slope.

© 2003 Elsevier B.V. All rights reserved.

Keywords: Soil erosion; Tracer; Sediment; Rare earth element; Sediment transport

* Corresponding author. Ohio State University, School of Natural Resources, 422D Kottman Hall, 2021 Coffey Road, Columbus, OH 43210-1085, USA. Fax: +1-614-292-7432.

E-mail address: polyakov.1@osu.edu (V.O. Polyakov).

1. Introduction

Soil erosion is a global environmental problem, which is often easy to observe but hard to measure. For example, annual soil loss on US cropland has been reported to be between 2 billion tons (USDA, 1980) and 6.8 billion tons (Harlin and Barardi, 1987). Soil conservation efforts require large investments, which put special importance on technology capable of correctly estimating erosion rates and precisely identifying problem areas within watersheds. The key to determining the extent of erosion lies in proper modeling, evaluation and monitoring techniques.

One monitoring technique is the tagging of soil with tracers. Tracers have been successfully utilized in the natural sciences to study transport processes and the fate of various pollutants. There are a number of substances that may be used for this purpose. They can be classified as naturally occurring and artificially introduced into the soil. Artificial tracers are either introduced into the soil as a result of fallout (e.g., ^{137}Cs) (Ritchie and McHenry, 1990) or deliberately, either by tagging soil particles with trace elements (e.g., noble metals, ^{59}Fe) (Wooldridge, 1965) or by incorporating trace particles into the soil body (e.g., magnetic and glass beads) (Ventura et al., 2001). The ideal use of tracers for monitoring soil translocation should be based on the following assumptions (Di Stefano et al., 1999): (1) the local distribution of the tracer is uniform (or not uniform, but known), (2) the tracer binds strongly with soil, (3) subsequent redistribution is due to sediment movement and (4) estimated erosion rates may be derived from tracer inventories.

Of all soil tracers, ^{137}Cs has been used most extensively (Ritchie and McHenry, 1990; Di Stefano et al., 1999). It has been suggested that ^{137}Cs is retained mostly by clay particles (He and Walling, 1996). Because vegetation retention and uptake of ^{137}Cs is low (Garten et al., 1975), its redistribution is mostly attributed to soil movement. There are a number of problems associated with the use of ^{137}Cs as tracer. Its fallout occurred in a complex temporal pattern. The basic assumption that fallout of ^{137}Cs is uniform over a study area is often unacceptable (Sutherland, 1994a). Nonuniform distribution is related to topography, soil density and infiltration (Di Stefano et al., 1999). In many areas, Chernobyl fallout increased the nonuniformity even more (Di Stefano et al., 1999). Due to the short half-life of ^{134}Cs , which initially accompanied Chernobyl ^{137}Cs in a strict proportion, Chernobyl ^{137}Cs will soon be indistinguishable from previous fallouts in the affected areas (De Roo, 1991). According to Sutherland (1994b), to adequately quantify the reference ^{137}Cs activity for an area with an allowable error of 10% with 90% confidence, approximately 11 random, independent samples will generally be necessary. The median coefficient of variation (CV) for ^{137}Cs reference activity on undisturbed soil reported in the literature, as cited by Sutherland (1994b), was 19.3%, with 95% confidence limits of 13.0–23.4%. Wallbrink et al. (1994) reports CVs for ^{137}Cs inventories within Australia as high as 40%. A CV for ^{137}Cs activity of 16%, with an allowable error of 10% at 95% confidence level, reported by Bernard et al. (1998) for a watershed in France, was well below numbers usually found in many studies. Such variability, if it is random, makes it impossible to use ^{137}Cs to detect soil movement on an event basis. Even detecting soil losses over a period of several years would be problematic (Kachanoski and DeJong, 1984). Preferential adsorption of ^{137}Cs on fine clay particles makes it prone to sorting during transport by

water. Bernard et al. (1998) reported the enrichment ratio for this tracer varying between 1.8 and 3.0.

^7Be and ^{10}Be are naturally occurring radionuclides of cosmogenic origin with a high affinity to clays. This element has large spatial variability because of interception by vegetation. Beryllium was used with ^{137}Cs (Matisoff et al., 2002) and alone (Wallbrink and Murray, 1996) to develop quantitative models of soil erosion and describe soil redistribution properties. Due to the differences in distribution and depth of penetration, the combination of two tracers, ^{137}Cs and ^7Be (Wallbrink and Murray 1993) or three tracers, ^7Be , ^{137}Cs and ^{210}Pb (Whiting et al., 2001), allows one to make inferences about the types of predominant erosion processes (rill or sheet) that have been active in sediment source areas. ^{10}Be is especially suitable for long-term estimates due to its long half-life (Brown et al., 1988). To preserve the properties of the material under study, several nondestructive labeling techniques have been developed. The radioactive ion ^{59}Fe in solution has been applied directly into soil (Wooldridge, 1965), and ^{60}Co has been used to tag stable soil aggregates consequently incorporated into soil (Toth and Alderfer, 1960). Both tracers were retained in silt and clay fractions. Wheatcroft et al. (1994) and Olmes and Pink (1994) employed thermal diffusion to introduce noble metals into the crystalline lattice of clay minerals with subsequent leaching of the excessive tracer. Particle size of sediments was not affected by these procedures, thus minimizing the error usually associated with tracer enrichment. However, this method is relatively complex and costly.

Yet, another way to trace soil movement is to introduce foreign particles. Fluorescent dyes, incorporated into 44- to 2000- μm glass particles (Young and Holt, 1968), were used under simulated rainfall on 4×10 m plots. Soil movement was detected, including splash movement and runoff. Wheatcroft (1991) used plastic beads to study horizontal mixing due to bioturbation. Plante et al. (1999) successfully tested ceramic pills with dysprosium. Ceramics simulate soil aggregates better than glass or plastic because of their density. Magnetic tracers made of plastic with imbedded magnetite (Ventura et al., 2001) and steel nuts (Borselli and Torri, 2001) allowed quick detection with a magnetometer in the field without lengthy laboratory analysis. The latter method is only applicable for translocation of soil by tillage operations and on limited areas. Fly-ash, a product of fossil fuel burning, primarily coal, was found to be useful in soil loss determination (Hussain et al., 1998; Olson et al., 2002) when comparing its amount in the soil profile at different landscape positions on a cultivated field and reforested site. Fly-ash primarily consists of siliceous glass with less-than-20- μm particle size. The common problem of using foreign particles as tracers is the difficulty to adequately represent the texture and aggregate size distribution of the studied soil as well as its specific weight. Hence, underestimation or overestimation of soil loss from sorting of tracers by water is essentially inevitable.

The lanthanides or rare earth element (REE) group consists of 15 elements with periodic number 57 through 71, of which one (Pm) is unstable and does not occur naturally. Lanthanide's trivalent state and ionic radiuses ranging between 0.861 Å (Lu^{3+}) and 1.03 Å (La^{3+}), similar to that of Ca^{2+} , allow them to be easily adsorbed to clay (Mahler et al., 1998). Similarity of ionic radii within the group, which decreases systematically with mass, ensures homogeneity of their chemical and physical properties in comparison with other groups of ions. They are found in many soils in concentrations of up to tens of

parts per million (Markert, 1987) with organic soils usually richer in lanthanides than mineral soils. REEs with even atomic numbers are always more abundant in nature than the adjacent elements with odd atomic numbers. Rare earth compounds show low toxicity ratings and often are accumulated by plants through roots (Wytenbach et al., 1998), although the uptake is too low to cause considerable change in concentration of REE in soil. REEs occur in a variety of minerals, such as monazite, apatite and titanite. The solubility of these elements tends to increase with decreasing pH, which is a key factor in their mobility in soil (Land et al., 1999).

REEs are often used in different areas of biological, environmental and earth sciences dealing with mass transport such as sediment transport. Krezoski (1989) used REE oxides to trace sediments in Lake Superior. Lateral transport of sediment and tracer were detected. Mahler et al. (1998) successfully tested lanthanide-labeled clay to characterized mass transport in karst. The potential of REE as a soil tracer is great. In a study by Zhang et al. (2001), REE oxide powder showed strong binding with a silt loam soil, low mobility, uniform distribution among aggregates of various sizes and low detection limits. Application of REE on agricultural soils is limited to a few pioneering studies both in the laboratory under simulated rainfall (e.g., Zhang et al., 2003) and on the field (e.g., Matisoff et al., 2001; Tian et al., 1994). Zhang et al. (2003) used five REE elements applied in 0.15-m bands across the slope in a 4×4 m laboratory plot with a silt loam soil. The authors reported 14.5% relative error of soil loss estimation by REE method compared with the direct measure of soil loss. Also, spatial distribution of erosion and deposition was observed in that study.

REEs are relatively easily detected with inductively coupled plasma mass spectrometry (ICP-MS). They reasonably satisfy a set of properties needed for an ideal tracer as defined by Zhang et al. (2001), namely: strong binding with soil, sensitivity to analysis, ease of measurement, low background concentration in soil, no interference with soil movement, chemical stability and low plant uptake, environmental safety and availability of multiple tracers with similar properties. The last of the listed properties enables the scientists to study sources and sinks of sediments from various areas of the field or plot.

The aim of the study was to develop and evaluate a practical soil tracing method that would allow quantitative evaluation of spatial and temporal soil erosion distribution. The specific objectives were: (1) to test the performance of rare earth element oxides as soil tracers and (2) to develop a technique for tracer application.

2. Materials and methods

2.1. Soil characteristics

The soil used in the study was Camden silt loam (fine-silty, mixed, mesic Typic Hapludalf) with 17% clay, 76% silt, and 7% sand content. It was collected southwest of West Lafayette, Tippecanoe County, IN. The soil is formed in late-Wisconsinian loess. It is dark colored, deep and well-drained with rapid permeability. Primary particle size distribution was determined using the pipette method (Franzmeier et al., 1977). A sodium metaphosphate and sodium carbonate solution was used as the dispersing agent. The soil

was air-dried in the laboratory and all fractions, which passed through an 8-mm sieve, were used in the experiment.

2.2. Experimental plot

To conduct the experiments, a $4 \times 4 \times 0.8$ m wooden experimental box was constructed (Fig. 1). One wall of the box was made 30 cm tall with two triangular funnels attached to collect runoff samples. The box was watertight and equipped with a drainage system. The drainage network consisted of 25 inlets located at the box floor and arranged in a 5×5 square grid pattern with 0.8 m spacing. The box was filled with sand, with the sand surface at 10% slope. The depth of the sand layer varied between 15 cm at the outlet to 55 cm at the upper part of the slope. Soil was spread on top of the sand in a uniform layer of approximately 15 cm. Average soil bulk density was 1.3 g cm^{-3} . Four programmable rainfall simulator troughs (Foster et al., 1979) were located 3 m above the soil surface (Fig. 2).

2.3. Laser scanner and operating procedure

A 4×4 m laser scanner, developed and built at USDA-ARS, National Soil Erosion Research Laboratory, was utilized to obtain digital elevation models (DEMs) of the soil surface. Laser scanner and control equipment consisted of a photodiode array mounted on a photo camera, digital input/output board, motor-driven X–Y traversing frame with step motors, motor controllers and diode laser. The diode laser had power of 3.48 mW and produced a light beam of 638.7 nm wavelength. A PC was used for scanner operation and

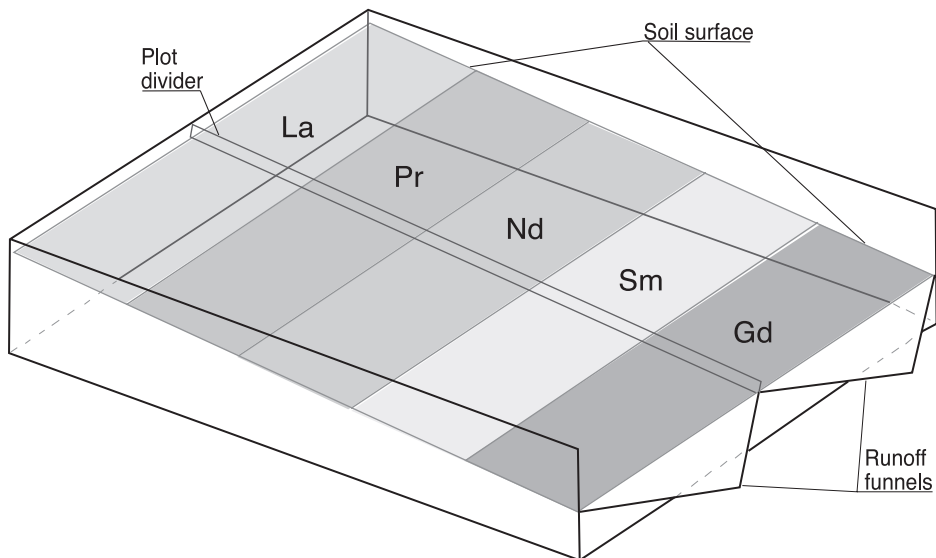


Fig. 1. Experimental soil box used in the study and tracer application scheme. The plot is divided on five zones each labeled with a tracer.

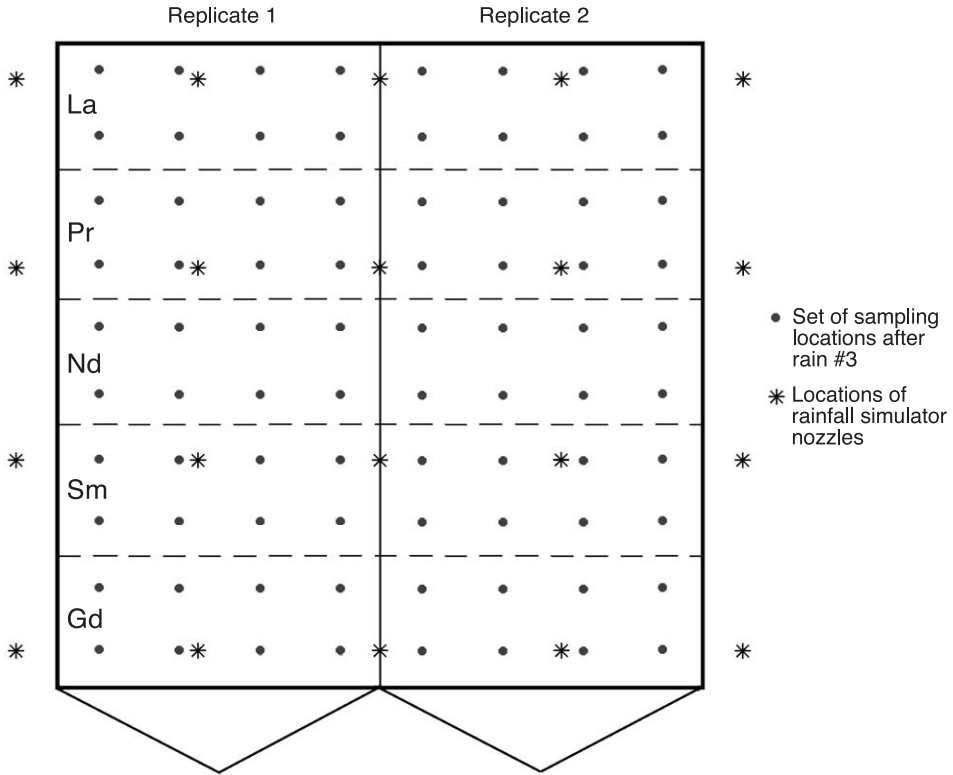


Fig. 2. Locations of core sample sites and rainfall simulator nozzles. The nozzle spacing was 1.15 m between adjacent simulator troughs and 1.1 m within a trough.

data logging. The prototype of the scanner and its operation procedure are described in detail by Huang and Bradford (1990) and Flanagan et al. (1995).

Resolution of scanning in the horizontal direction was set to 6×6 mm, which produced over 440,000 elevation points for the entire plot. Vertical resolution ranged between 0.2 and 0.3 mm depending on the distance from camera to the measured surface. Standard deviation of vertical measurement on a smooth surface was 0.13 mm. The scanner frame was installed at a 9% angle almost parallel to the slope to minimize the range of distances between scanner and soil. This allowed configuring the camera and the laser source to increase the precision of measurements by using only the middle part of the photodiode array.

To provide reference elevations for the DEMs, four aluminum brackets were attached to the walls in four corners of the box. Before each scan, elevation of these reference points was measured to account for possible movement of the scanner frame between runs. The scanner was calibrated to provide a conversion equation (second-order polynomial) from raw data measurement to relative elevation data.

Arc-View GIS software (ESRI, 1999) and in-house computer programs were used for conversion of raw measurement to elevation. Missing data points were linearly interpo-

lated using the closest adjacent DEM grid points in the direction of the slope. DEMs produced after consecutive rainfalls were subtracted from each other to obtain spatial distributions of soil loss and gain on the plot.

2.4. REE properties and preparation of tracers

Five rare earth element oxides in powder form were used as tracers in the study (Table 1). In order to uniformly apply each of the REEs on separate portions of the experimental plot, a soil–tracer mixture was prepared. Air-dried soil (10 kg; same as on the plot) was passed through a 2-mm sieve. The target REE concentration on the plot after tracer application was set to be 10 times that of the background level. Amounts of REE oxides needed to tag 1/5 of the plot area to the depth of 4 cm were weighed, and each aliquot was mixed with 2 kg of soil. It was presumed that soil loss during the experiment would not exceed 4 cm application depth. Then the mixture was wetted, stirred and air-dried to prepare it for application. The wetting and drying cycle was intended to help incorporate the tracer powder into the soil aggregates, as well as to prepare the mixture for spreading.

2.5. Experimental procedure

Because erosion varies as a function of slope length, in order to determine soil losses at various slope positions, the plot area was subdivided into five 0.8-m strips stretching across the slope. Each strip was tagged with its unique tracer: La, Pr, Nd, Sm and Gd (Fig. 1). The soil–tracer mixture was spread on the plot using calibrated Scotts® AccuGreen® 1000™ lawn spreader with a 40-cm-wide span. During the application, the soil adjacent to the strip was covered with plastic to prevent accidental contamination of adjacent areas. Then, the top 4-cm layer of soil with tracer mixture on it was thoroughly mixed using a hand roller-cultivator. Care was taken to prevent the transfer of soil from one strip to another during mixing. The soil box was then divided into two equal parts by metal plates inserted into the soil along the slope (Fig. 1). This was done to create two replicated plots 2 m wide and 4 m long each.

Prior to the first run, the soil was allowed to wet slowly to a saturated condition for 24 h. This was achieved by running water over the soil surface protected by perforated plastic. Care was taken to ensure that the water saturating through the perforated plastic caused no soil incision. Eight consecutive 1-h-long rainfalls at 60 mm h⁻¹ intensity were conducted

Table 1
Selected properties of the five REE oxide tracers used in the experiment

Element	Oxide	D_{50} , μm^a	Specific gravity, g cm^{-3a}	Background in soil, ppm
Lanthanum	La_2O_3	1.23	6.51	17.2
Praseodymium	Pr_6O_{11}	16.38	6.83	4.4
Samarium	Sm_2O_3	3.61	7.68	3.6
Gadolinium	Gd_2O_3	2.19	7.41	3.0
Neodymium	Nd_2O_3	3.65	7.24	16.8

^a Data from Zhang et al. (2001).

with a 3-day period between runs. The soil surface was left intact between rainfall simulations. After each rainfall, a DEM of the plot surface was measured with the laser scanner.

Thirty 1-l runoff samples were collected at 2-min intervals during each 1-h run from each of the two replicates. These were used to determine water and sediment discharge. Aluminum potassium sulfate was added to the samples to flocculate and settle suspended sediments. After the settling, the excess water was poured out and the sediments were dried at 105 °C. Samples were weighed to determine total sediment yield from the soil bed. After this, sediments in the runoff samples were used to determine REE concentration. Due to the complexity and cost of the chemical analysis, six consecutive samples taken at 2-min intervals were mixed to produce five combined samples per run. These combined samples, each representing 12 min of runoff, were ground and thoroughly mixed.

Surface samples were collected with a cylindrical auger 13 mm in diameter to a depth of 3 cm. Thus, the depth of the sampling did not exceed the depth of the vertical tracer distribution. It ensured that the sample was not diluted by the soil untagged by REE tracers. At the same time, the sampling depth was great enough to penetrate through the layer of deposited soil where sedimentation occurred. Samples were located in a grid pattern with a spacing of 0.4 m between rows and 0.5 m in row (across the slope). After each rainfall the sampling grid was slightly shifted such that no new sample hit the spot disturbed previously. Four samples from each row were combined to make a composite sample that represented a 40-cm-wide horizontal band of the slope.

2.6. REE extraction and analysis by inductively coupled plasma mass spectrometer

Samples were prepared for ICP-MS analysis using the extraction procedure modified by Zhang et al. (2001) from USEPA standard method for extractions of metals from environmental samples (USEPA, 1995). Two grams of soil was placed into a 50-ml flask and 10 ml of concentrated HNO₃ (70% wt.%) was added, and the mixture refluxed for 2 h in a water bath at 85 °C. After cooling to <70 °C, 10 ml of H₂O₂ (30%) was slowly added to remove organically bound REEs. The solution was then brought to 85 °C until effervescence subsided. Five milliliters of concentrated HCl (36 wt.%) was added, and the solution again refluxed for 2 h in a water bath at 85 °C. After cooling to room temperature and a 24 h waiting period, the solution was filtered through filter paper with particle retention >2.5 μm, and eluted with 5 ml deionized H₂O (18 MΩ cm⁻¹). Then the solution was filtered through a 0.45-μm membrane and transferred to 50-ml centrifuge tubes. Samples were analyzed for La, Pr, Sm, Gd and Nd by ICP-MS at the Purdue University Department of Chemistry. Stock internal In and Tl standards were used. Samples were diluted and three replications were made. The average coefficient of variation of REE concentration determination was 4.5%.

2.7. Runoff and surface sample analysis

Concentrations of tracers in samples were compared to the background and application levels. Increased amount of tracer in the surface samples indicated depositional areas or

sinks, while such an increase in the runoff samples indicated that the area labeled with corresponding tracer was the sediment source.

The proportional method used in the analysis was based on the assumption that the concentration of the tracer in bulk soil is equal to the concentration of that in eroding soil:

$$L_i = L_t(C_{mi} - C_{bi}) / (C_{ai} - C_{bi}) \quad (1)$$

where L_i is the soil loss from area with i th tracer (kg), L_t is the total soil loss (kg), C_{mi} is the measured tracer concentration in sediment yield (ppm), C_{bi} is the background concentration (ppm) and C_{ai} is the application concentration (ppm). Some sediment after detachment could have been redeposited on the lower part of the slope. Soil movement on the slope can be accounted for by analyzing the surface samples using:

$$D_x = \sum((C_{mi} - C_{bi}) / (C_{ai} - C_{bi})m / A) \quad (2)$$

where D_x is the deposition at location x of the slope (kg m^{-1}), m is the mass of the sample (kg) and A is the area of the sample (m^2). Complete sediment balance was obtained by combining soil loss calculated from runoff samples and deposition determined from surface samples. Analysis of the acquired data was performed using ArcView 3.2 GIS software (ESRI, 1999) and statistical software SAS 6.12 (SAS Institute, 1990). A 95% probability level was used in statistical analyses throughout the study.

3. Results and discussion

3.1. Rainfall and runoff patterns

Rainfall intensity measured at nine locations on the plot was 63 mm h^{-1} with a coefficient of variation of 7.4%. Runoff started 8 min after initiation of the first rainfall and increased rapidly until it reached a steady rate after 50 min. During the following seven rainfall events, runoff reached a steady rate after the first 5 min.

Soil matric potential gradient and surface sealing were among the factors that significantly influence infiltration rate and, as a result, runoff. The prewetting of the soil to a saturated condition before the simulation began reduced the effect of the matric potential gradient on the initial infiltration process, which could have been significant in dry soil, and also prevented the soil from slaking. Under these circumstances, the decline in the infiltration rate (and increase of the runoff) during the first rain event was primarily the result of soil structural deterioration. Raindrop impacts caused soil aggregates to break down, disperse and block soil pores. A surface seal developed and the soil surface underwent the process of smoothing and compaction. During rain events 2 through 8, the steady state conditions (7.5 and 7.2 l min^{-1} on plots 1 and 2, respectively) were reached within the first 5 to 10 min of each simulation. This was the time required for the runoff to accumulate and reach the outlet. The infiltration rate at saturated conditions was 8 mm h^{-1} , or 12% of the precipitation rate.

3.2. Spatial distribution of erosion

Soil erosion is a spatially variable phenomenon. Both sheet and rill erosion was observed on the plot. Visible rills started to develop after approximately 3 h (180 mm) of rainfall and continued to increase afterwards. It was important to know the magnitude of this process, because possible contribution of soil from deeper layers (untagged by tracers) to runoff would lead to the underestimation of soil loss by the REE method. To estimate the relative contribution of sheet and rill erosion to the total sediment yield, we investigated the frequency distribution of soil loss depth on the plot. These frequencies were obtained from the DEMs of the soil surface.

The histogram on Fig. 3 presents the frequency distribution of soil loss depth on the plot and the change in this distribution as a function of cumulative rainfall. The depth of soil loss was grouped into 4-mm classes. After the second rain event (120 mm of cumulative precipitation), areas of soil loss 0–4 mm deep were the most frequently occurring (90% of the plot area), while only 1% of the plot area (Fig. 3) had soil loss greater than 8 mm deep. After the eighth rain event (480 mm of precipitation), 90% of the plot experienced soil loss less than 16 mm deep, which accounts for over 80% of soil loss by mass.

The frequencies of occurrence of soil loss depth classes for all rain events were normally distributed. The mode (most frequently occurring value) of the distribution increased with cumulative rainfall and after the 8th rain event was in the 4- to 8-mm-deep soil loss class. At the same time, the range of the soil loss distribution also increased (Fig. 3). These trends suggest that during the first two rain events the soil loss depth was relatively uniform across the plot. During the subsequent rain events, the rills began to

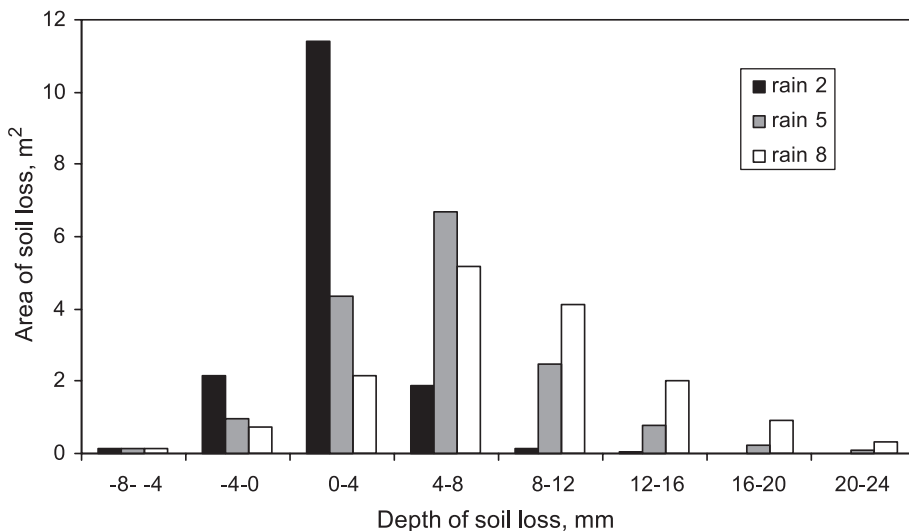


Fig. 3. Frequency distribution of soil loss depth on the plot and the change in the distribution with cumulative rainfall. Values were determined from the DEMs obtained by the laser scanner.

cover an increasingly larger area of the plot. Also, the area where net deposition occurred (negative depth values in Fig. 3) decreased from 15% to 7% of the plot between the 2nd and 8th rain events. Initially, the tracers were mixed with the soil to a depth of 40 mm. Most of the plot area was affected by sheet erosion of much lesser depth. Rills did not penetrate through the REE-tagged soil layer and did not effect the assessment of soil loss by REE.

3.3. Estimation of soil loss using a digital elevation model

Digital elevation models obtained by scanning the soil surface between rainfall events provided a reference measure of net soil loss with a high spatial resolution. The number of error readings did not exceed 0.52% for any single scan and was 0.29% on average for all scans.

The channel network propagated from the outlet and grew upslope along the lines of concentrated runoff. Several major channels developed headcuts, which propagated upstream and disappeared after approximately 300 mm of cumulative precipitation. Once the channels became incised, very little meandering occurred. Channels were broad and shallow and, by the end of the experiment, stretched up approximately two-thirds of the plot. In addition to the rill flow, shallow overland flow was present on all parts of the slope.

Soil compaction as a result of rainfall was observed during the first simulation. Bulk density of soil at the surface increased due to raindrop impact and destruction of soil aggregates. Also, compaction of the deeper soil layers might have occurred under the influence of water movement through the soil profile. This resulted in overestimation of soil loss by DEM after the first rain. This overestimation was corrected by relating loss measured by DEM and actual amount of sediment measured at the outlet.

The DEM of the soil surface change as a function of rainfall revealed a nonuniform soil loss pattern (Fig. 4). The nonuniformity of soil loss was the result of three factors: slope position, uneven rainfall distribution and rill incisions. Areas under the simulator troughs were subject to an increased erosion rate (areas of greater soil loss stretching across the slope on Fig. 4). Deposition occurred mostly near the outlet (Fig. 4) during the first three to four rainfalls, after which this area remained relatively stable in terms of the net amount of deposited sediment.

Measurement of soil loss using DEM is conceptually different from deriving it using tracer data. The scanner measures net change (erosion+deposition) on a particular location. Deposition measured from the REE is difficult to relate to the deposition derived from the DEM. For example, sedimentation may occur on the area where soil loss had taken place within the course of the same rainfall event. This soil replacement would be detected by the REE method as sedimentation, but on the DEM, the location may appear unchanged. Fig. 5 presents DEM-derived net soil loss from five REE-tagged sections of the slope as a function of precipitation. After 480 mm of rain, the most severe soil losses, 7.1 and 6.6 mm, occurred on the middle (Nd, 1.6–2.4 m) and upper-middle (Pr, 0.8–1.6 m) sections of the slope. These were equivalent to the loss of 9.3 and 8.6 kg m⁻¹ of soil on each of these sections, respectively. The uppermost section, La (0–0.8 m), and the two lower sections, Sm (2.4–3.2 m) and Gd (3.2–4.0 m), respectively lost 30%, 40% and 60% less soil than the Nd section.

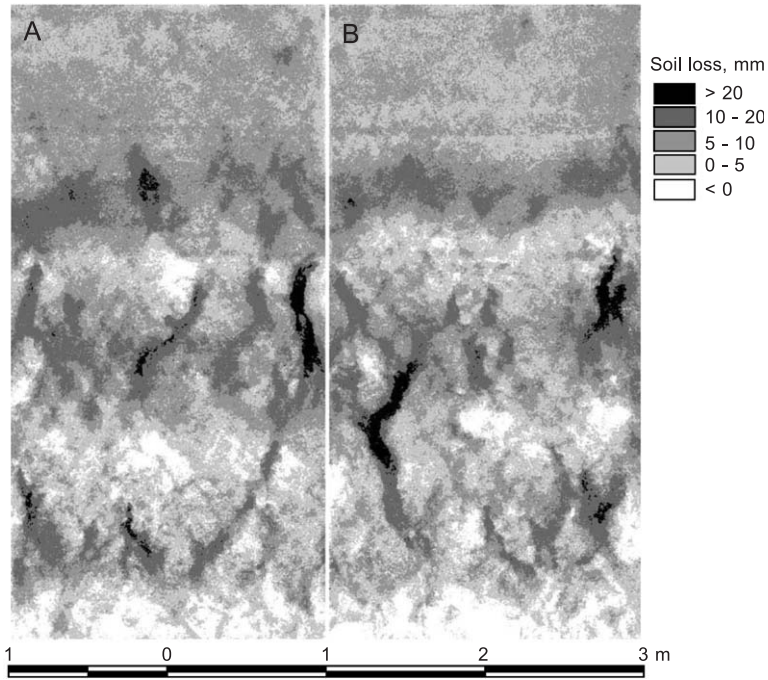


Fig. 4. Erosion and deposition pattern on the replicated plots 1 (A) and 2 (B) after six simulated rains (360 mm of cumulative precipitation). The plot outlet is at the bottom side of the map.

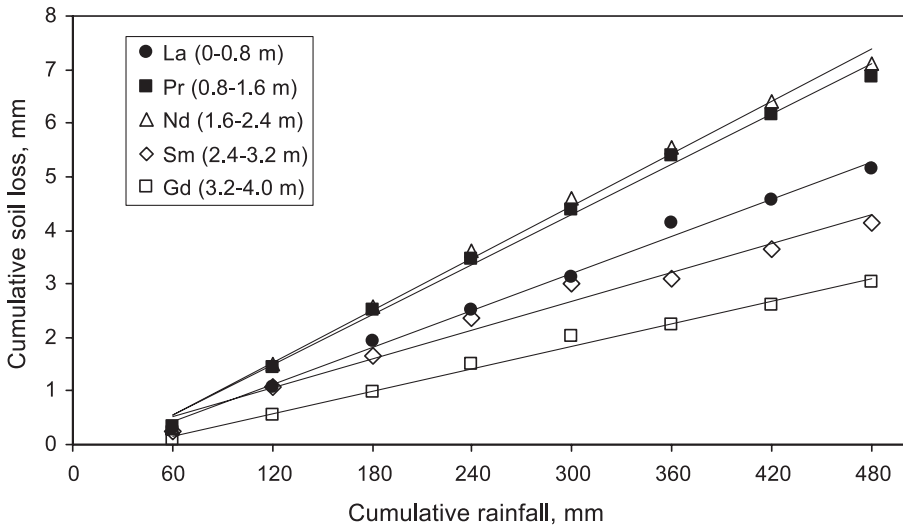


Fig. 5. The rate of net soil loss with cumulative rainfall on five REE-tagged sections of the plot as measured from the DEMs.

A relatively small net soil loss on the lower parts of the slope, together with the fact that the same area was characterized by the greatest flow accumulation, indicates that transport limiting conditions existed there and that deposition occurred. Another explanation for the observed spatial erosion pattern might have been the difference in relative contribution of rill and sheet erosion to the total sediment yield. The upper part of the slope had a relatively undeveloped rill network, and sheet erosion was dominant there. The rate of sheet erosion increased in the downslope direction as a result of gradual flow accumulation. However, on the lower half of the slope, rills began to play a more important role in transporting runoff and sediments. The flow from the upper portions of the slope was diverted to channels. Interrill areas on the lower part of the slope had relatively small contributing areas and, as a result, low erosion rates. Interrill areas on the lower portions of the slope were not severely eroded and even experienced deposition (Fig. 4). Yet, another reason for sediment accumulation on the lower slope position was the effect of plot end. While most of the plot surface was eroding, soil loss in the area adjacent to the outlet was controlled by the fixed elevation of the outlet funnel.

Throughout the rainfall simulations, the rates of soil loss (mm of soil per mm of precipitation) on all sections of the plot were constant (Fig. 5). Linear regression fitted to the plots gave coefficient of determination of 0.99 for all sections, except for the Sm (2.4–3.2 m), where r^2 was 0.97. Dimensionless soil loss rate was the greatest at the Nd section (1.6–2.4 m), measuring 0.016 mm mm^{-1} , followed by section Pr, La, Sm and Gd with corresponding rates of 0.015, 0.012, 0.009 and 0.007 mm mm^{-1} . These erosion rates (greater on the midsections and smaller on the upper and lower sections) caused the lower portion of the slope to level off, while making the upper part of it steeper, leading to formation of a slightly concave shape.

3.4. Sediment and tracer enrichment

Enrichment of sediment yield by certain class of particles results from the preferential transport of these particles by the flow. Slight sediment enrichment occurred when the soil was eroded and transported out of the experimental plot (Table 2). Fine fractions such as clay and fine and medium silt in the eroded sediment showed a 2–3% increase, while the amount of coarse silt and sand decreased.

Median diameters of the tracers were 1.23, 16.38, 3.61, 2.19 and $3.65 \mu\text{m}$ for La_2O_3 , Pr_6O_{11} , Sm_2O_3 , Gd_2O_3 and Nd_2O_3 , respectively. Three of the tracers, Sm, Gd and Nd, fall

Table 2
Particle size distribution of undisturbed soil used on the experimental plot and sediment eroded from the plot

	D ₅₀	Particle size								
		μm				mm				
		<2	2–5	5–20	20–50	0.05–0.1	0.1–0.25	0.25–0.5	0.5–1	1–2
	μm	%								
Matrix soil	13.9	17.2	8.9	39.9	27.3	2.0	2.0	1.8	0.8	0.1
Eroded sediment	12.1	20.0	9.8	42.9	23.1	1.4	1.5	1.1	0.1	0.1

into fine silt range, Pr into medium silt and La into clay size range. Median diameters of all tracers, except Pr_6O_{11} , were three to four times lesser than those of both matrix soil or eroded sediments.

Although Zhang et al. (2001) reported that REE oxide powders, when incorporated into a silt loam soil, showed good binding and a relatively uniform distribution across different size of aggregates after wet sieving, a considerable enrichment of sediment with tracers was observed in our study. Tracer enrichment ratio is the ratio between concentrations of tracer in sediment to those in undisturbed soil. Tracer enrichment ratio different from 1 is the result of preferential transport of either soil or tracer. A plot of sediment discharge measured directly by weighing runoff samples and derived from REE (Eqs. (1) and (2)) reveals that the amount of sediment calculated using REE was overestimated (Fig. 6). During the first 30 min of simulation, the ratio between measured and calculated discharge reached as high as 3. This can be explained by initial flushing of the poorly incorporated tracer from the soil. By the end of the first rain, this ratio had decreased to 1.7 and remained steady during all consecutive runs with a coefficient of variation 7%. We hypothesize that the enrichment ratio of tracer depends on flow hydraulic conditions and distance from the source, however, this relationship is difficult to measure. The value 1.7 was used in further calculations as an average correction coefficient.

A process of initial overestimation of sediment discharge by REE method and decrease of the tracer enrichment ratio with cumulative rainfall was reported by Zhang et al. (2003) in a similar study. The authors used REE placed on the plot in narrow bands. In that case, after 60 mm of precipitation, the enrichment ratio fell from 1.97 to 1.2 and continued to decrease, reaching 1.04 after six rain events. The enrichment process has also been reported for other tracers. For example, for ^{137}Cs , it varies from 1.1 (He and Walling, 1996) to as high as 3.0 (Kachanoski, 1993).

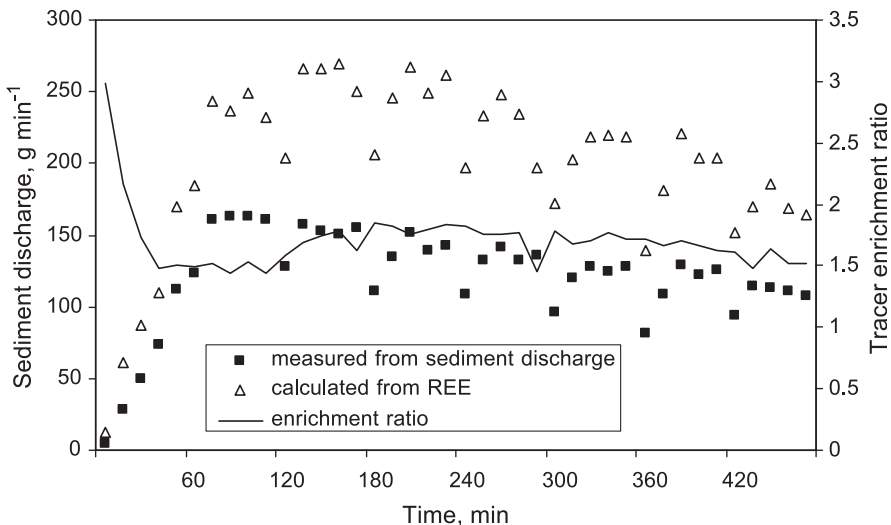


Fig. 6. Relationship between sediment discharge from the plot estimated using REE and directly measured from runoff samples.

Our data, as well as previous findings, indicate that the enrichment ratio is sensitive to the condition in which the experiment is conducted, soil and tracer properties and the technique of their application. Because no single tracer can adequately represent the whole range of soil aggregates and particle sizes, enrichment must be estimated and accounted for. However, the binding of powder REE oxides with the soil might be improved if a different incorporation technique is used. Also, application of REE in the form of a solution might improve binding.

3.5. Deposition on the plot

The pattern of sediment deposition of four tracers on downslope sections after 480 mm of rain, as determined from REE, is presented in Fig. 7. Sedimentation of the fifth tracer (Gd) could not be measured because it was adjacent to the outlet. Core samples represented cumulative deposition from all previous rains.

The largest portion of deposited sediments on the slope originated from the Pr section (0.8–1.6 m from the top of the plot). This area accounted for 40% of all deposition and it also had the greatest sediment yield. Average deposition from a section per unit area was roughly proportional to its loss to runoff. Fig. 8 shows the dynamics of the deposition as a function of cumulative rainfall from individual sections on area downslope. Most of deposition occurred during rains 1 and 2. A portion of the deposition may have been removed during rain 4. This is indicated by the decline in accumulation at 240 mm of cumulative precipitation. This might have been attributed to the development and widening of rills on the slope, or it could be due to variability in the samples. The stabilization of the amount of deposited sediments after rain 6 (Fig. 8) indicated that quasi-steady detachment–deposition conditions were reached.

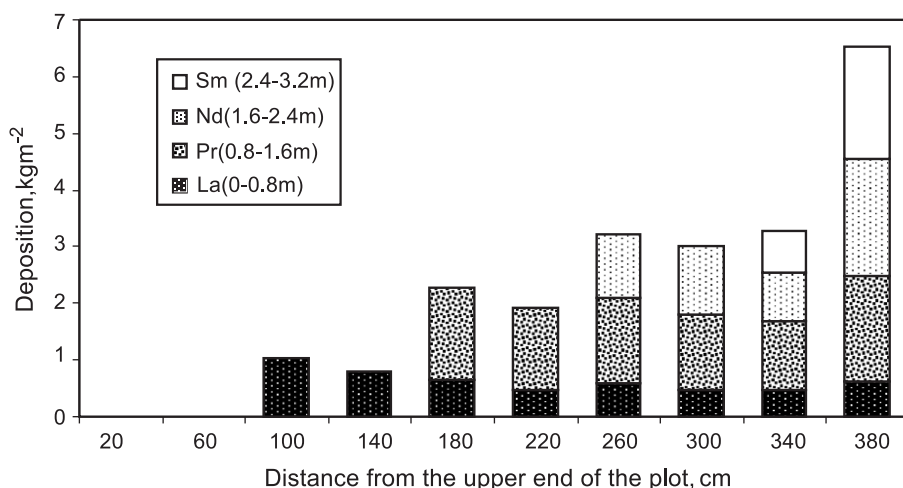


Fig. 7. Spatial distribution of soil deposition. Gradation of gray represent different sources (four uppermost sections of the plot) of the deposited soil. Average between the two replications after eight simulated rains (480 mm of precipitation).

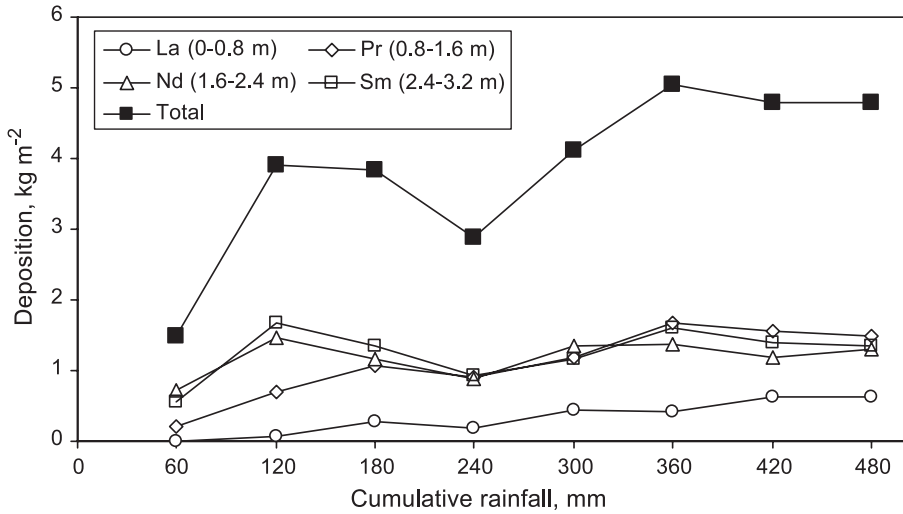


Fig. 8. Cumulative deposition of soil eroded from the four uppermost sections of the plot on the area downslope (sum of the two replicates).

3.6. Total sediment balance

The spatial patterns of soil loss measured using DEM and that estimated by tracers agreed relatively well (Fig. 9). The DEM-derived data were obtained by subtracting the DEMs of eroded and the initial (before the simulations) soil surfaces from each other, thus calculating the volume of eroded soil (taking into account the soil density changes after the

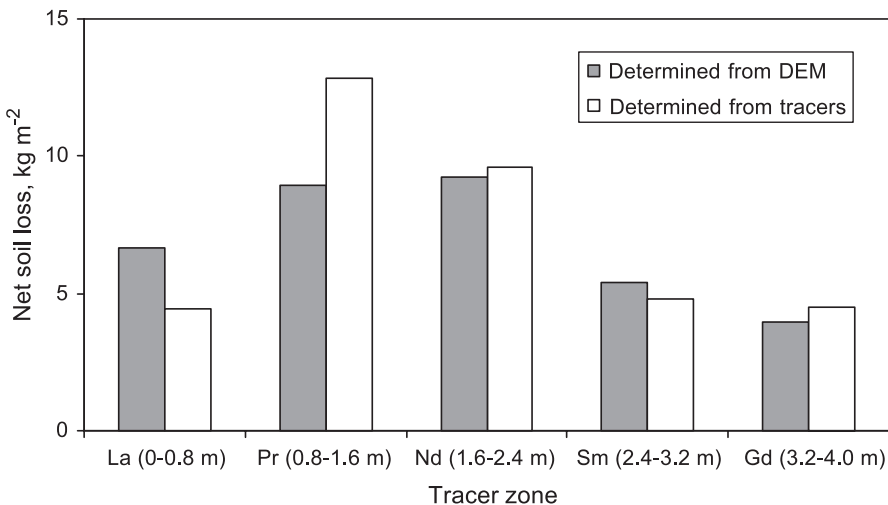


Fig. 9. Total net soil loss on five REE-tagged sections of the slope as determined from DEMs and estimated using REE tracers (sum of the two replicates after eight simulated rains, 480 mm of precipitation).

first wetting). The soil loss by the REE method was calculated using Eq. (1) (the proportional method). In addition to this, redeposition on the lower parts of the slope as well as sediment input from the higher locations was accounted for using Eq. (2). Finally, the result was adjusted using an enrichment correction value of 1.7 described earlier. Net erosion on the Pr section of the slope (0.8–1.6 m) was overestimated by 40% compared to the DEM data. The largest underestimation (30%) occurred on the uppermost section. The soil loss estimates by the two methods on the other three sections (Nd, Sm and Gd) differed by less than 13%. The differences between the estimates by the two methods were not statistically significant, except for the upper slope section (La, 0–0.8 m).

Estimation of soil loss from sediment sources located further from the outlet to a greater degree depended on accurate measurements of deposition. Due to the REE extraction and analysis constraints, the number of surface samples was limited. The precision of the deposition measurement could have been improved if each combined sample contained a greater number of subsamples. Also, an irregular sampling scheme could have been used instead of a square grid pattern. Random sampling is usually preferable in the situations where the sampled phenomenon has spatial regularity (Isaaks and Shrivastava, 1989). This may have been the case in the present study where evenly spaced rainfall simulators produced somewhat systematic rainfall pattern.

The sediment budget at a point on the slope consisted of three components: (1) soil that was eroded from the point and exported from the plot; (2) soil that is eroded from the point and deposited downslope; and (3) soil deposited at the point. Breakdown of the sediment budget on these components is presented in Fig. 10 and Table 3. Our results suggest that detachment and deposition processes on the slope occurred simultaneously (Fig. 10; Table 3). For example, while on the section Nd (1.6–2.4 m) after the 8th rain, a loss of 10.9 kg

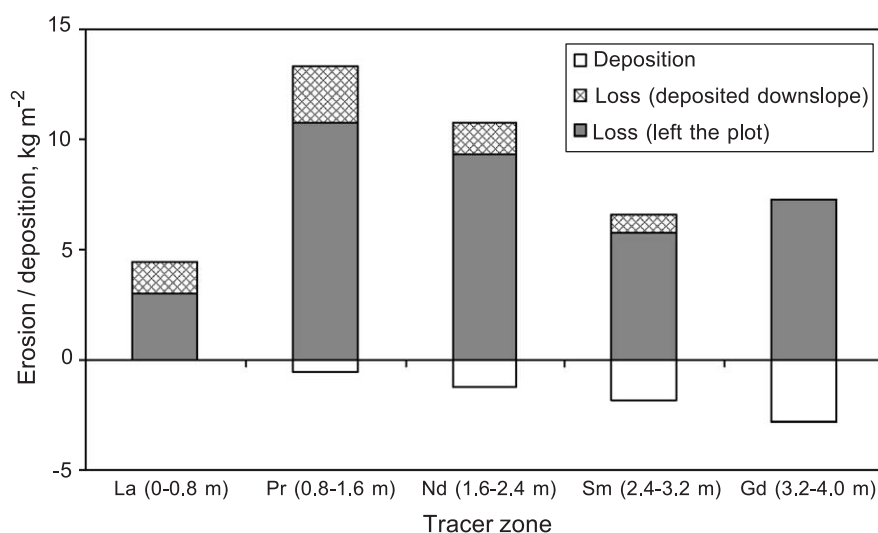


Fig. 10. Soil translocation on five sections of the slope after eight simulated rains (480 mm of precipitation) as determined from REE tracers.

Table 3
Sediment balance and its components for eight rainfalls

	Slope element and its location					Average
	La, 0–0.8 m	Pr, 0.8–1.6 m	Nd, 1.6–2.4 m	Sm, 2.4–3.2 m	Gd, 3.2–4 m	
<i>Rain 1</i>						
Loss to runoff	0.05	0.26	0.33	0.38	1.00	2.02
Lost and redeposited	0.01	0.63	1.46	0.56		2.66
Gain		0.17	0.34	1.14	1.00	2.65
Balance	–0.06	–0.72	–1.45	0.20	0.00	
<i>Rain 2</i>						
Loss to runoff	0.46	1.84	1.76	1.39	2.36	7.81
Lost and redeposited	0.30	2.08	2.91	1.67		6.96
Gain		0.18	0.76	2.23	3.80	6.97
Balance	–0.76	–3.74	–3.91	–0.83	1.44	
<i>Rain 3</i>						
Loss to runoff	0.87	3.44	3.17	2.34	3.56	13.38
Lost and redeposited	1.09	3.18	2.30	1.35		7.92
Gain		0.33	1.74	2.32	3.53	7.92
Balance	–1.96	–6.29	–3.73	–1.37	–0.03	
<i>Rain 4</i>						
Loss to runoff	1.28	4.99	4.48	3.20	4.52	18.47
Lost and redeposited	0.75	2.69	1.75	0.92		6.11
Gain		0.18	1.63	2.05	2.25	6.11
Balance	–2.03	–7.50	–4.60	–2.07	–2.27	
<i>Rain 5</i>						
Loss to runoff	1.74	6.59	5.82	3.92	5.29	23.36
Lost and redeposited	1.75	3.53	2.71	1.16		9.15
Gain		0.72	1.64	2.64	4.14	9.14
Balance	–3.49	–9.40	–6.89	–2.44	–1.15	
<i>Rain 6</i>						
Loss to runoff	2.15	8.09	7.02	4.58	6.00	27.84
Lost and redeposited	1.65	5.00	2.74	1.61		11.00
Gain		0.43	2.35	2.24	5.96	10.98
Balance	–3.80	–12.66	–7.41	–3.95	–0.04	
<i>Rain 7</i>						
Loss to runoff	2.55	9.50	8.21	5.17	6.65	32.08
Lost and redeposited	2.51	4.69	2.38	1.41		10.99
Gain		0.82	2.60	2.21	5.35	10.98
Balance	–5.06	–13.37	–7.99	–4.37	–1.30	
<i>Rain 8</i>						
Loss to runoff	3.00	10.79	9.29	5.77	7.29	36.14
Lost and redeposited	2.56	4.48	2.61	1.36		11.01
Gain		0.91	2.09	3.11	4.89	11.00
Balance	–5.56	–14.36	–9.81	–4.02	–2.40	

Data are expressed as kg/m².

m^{-2} occurred, this section also experienced deposition of 1.6 kg m^{-2} . Zhang et al. (2003) explain such phenomena by the interrill–rill erosion concept, according to which most deposition occurs in the interrill area, while most of the detachment takes place in the rills. We recognize that such mechanisms might have taken place. However, it was indicated previously that the contribution of rill erosion to the total sediment yield was relatively insignificant. This suggests that detachment and deposition occurred simultaneously at the interrill locations on the slope.

We define sediment delivery ratio (SDR) as a ratio between the amount of sediment delivered to the outlet and the amount of sediment generated on hillslopes. The SDR after 8th rain was 0.85. This ratio varied among individual slope sections and depended on the location of the sediment source relative to the outlet. The ratio steadily decreased in the upslope direction. The La section had the lowest value of sediment delivery (0.67), followed by Pr, Nd and Sm with values of 0.81, 0.86 and 0.88, respectively.

The potential of multiple REE tracers to differentiate between the three components that comprise the sediment budget is particularly important. It allows estimating the rate of sediment movement along the slope and determining the sediment residence time in the system. This also can be used to study the fate of various pollutants associated with soil.

4. Conclusion

A laboratory experiment was conducted to test the performance of various REE oxides as soil tracers on different sections of the slope. The tracers allowed the detection and quantification of soil redistribution on the slope, as well as calculation of sediment yield from individual sections. The greatest soil loss occurred on the middle and upper-middle parts of the slope, which corresponded well with direct measurements by the laser scanner. Discrepancy of the soil loss estimates between that measured by the REE method and the laser scanner method varied between 4% on the lower slope and 40% on upper parts of the slope. This error was related to the large spatial variability of deposition, which mostly occurred near the outlet and comprised a substantial portion of soil removed from the upper sections. However, considering the variable nature of soil erosion such discrepancy in estimates might be acceptable.

The rate of the soil loss on each slope section was constant throughout the experiment and was linearly related to the amount of cumulative rainfall. A greater erosion rate was observed on the middle of the plot and lower rates on the upper and lower sections. This indicated that the lower part of the slope was leveling out, while the upper part was becoming steeper, leading to the formation of a concave profile. Most of the net deposition occurred during rains 1, 2 and 3 (180 mm of precipitation) and remained relatively stable during further rainfall. We hypothesize that the system was in a quasi-steady detachment–deposition condition after rain 3.

REE tracers were subject to sorting during transport, which may have been related to their fine texture and insufficient binding with soil aggregates or nonuniform binding to soil aggregates. The enrichment ratio of tracers was the greatest during the first rain and decreased during rains that followed to a steady value of 1.7. Though it was greater than

the 1.04 obtained by Zhang et al. (2003) for REE in a similar experiment, it is comparable with values of 1.1–3.0 reported for ^{137}Cs (He and Walling, 1996).

The REE tagging method offers a powerful and practical way to trace the movement of soil under erosive forces. It allows one to identify sources and sinks of sediment and itemize the sediment budget of any given location by its major components: sediment loss, deposition from upslope locations and redeposition on downslope locations. It is impossible to distinguish between the last two components using any other method, including single tracer methods. However, additional investigation may be needed to determine how soil properties, rainfall characteristics and tracer placement relative to the outlet influence the tracer enrichment ratio. Also, the feasibility of using lanthanide elements should be further studied at the field scale on complex landscapes and under natural rainfall.

References

- Bernard, C., Mabit, L., Wicherek, S., Laverdiere, M.R., 1998. Long-term soil redistribution in a small French watershed as estimated from Cesium-137 data. *Journal of Environmental Quality* 27, 1178–1183.
- Borselli, L., Torri, D., 2001. Measurement of soil translocation by tillage using a non invasive electromagnetic method. *Journal of Soil and Water Conservation* 56 (3), 106–111.
- Brown, E.T., Pavich, M.J., Hickman, R.E., Klein, J., Middleton, R., 1988. Erosion of the Eastern United States observed with Be-10. *Earth Surface Processes and Landforms* 13, 441–457.
- De Roo, A.P.J., 1991. The use of ^{137}Cs as a tracer in an erosion study in south Limburg (the Netherlands) and the influence of Chernobyl fallout. *Hydrological Processes* 5, 215–227.
- Di Stefano, C., Ferro, V., Porto, P., 1999. Linking sediment yield and Cesium-137 spatial distribution at basin scale. *Journal of Agricultural Engineering Research* 74, 41–62.
- ESRI, 1999. ArcView GIS Users Guide. Version 3.2. Environmental System Research Institute, Redlands, CA.
- Flanagan, D.C., Huang, C., Norton, L.D., Parker, S.C., 1995. Laser scanner for erosion plot measurements. *Transactions of the ASAE* 38 (3), 703–710.
- Foster, G.R., Eppert, F.P., Meyer, L.D., 1979. A programmable rainfall simulator for field plots. Proceedings of Rainfall Simulator Workshop, 7–9 March 1979, Tucson, AZ. USDA, Science and Education Administration, Agricultural Reviews and Manuals, ARM-W-10. USDA, Washington D.C., pp. 45–59.
- Franzmeier, D.P., Steinghardt, G.C., Crum, J.R., Norton, L.D., 1977. Soil characterization in Indiana: I. Field and laboratory procedures. *Research Bulletin* 943.
- Garten Jr., C.T., Gentry, J.B., Pinder III, J.E., Sharitz, R.R., Smith, M.H., 1975. Radioacecium dynamics in a contaminated flood plain ecosystem in the southeastern United States. Impact of Nuclear Releases into the Aquatic Environment. International Atomic Energy Agency, Vienna, pp. 331–347.
- Harlin, J., Barardi, G., 1987. *Agricultural Soil Loss*. Westview, Boulder, CO.
- He, Q., Walling, D.E., 1996. Interpreting particle size effects in the adsorption of Cs-137 and unsupported Pb-210 by mineral soils and sediments. *Journal of Environmental Radioactivity* 30, 117–137.
- Huang, C., Bradford, J.M., 1990. Portable laser scanner for measuring soil surface roughness. *Soil Science Society of America Journal* 54 (5), 1402–1406.
- Hussain, I., Olson, K.R., Jones, R.L., 1998. Erosion patterns on cultivated and uncultivated hillslopes determined by soil fly ash contents. *Soil Science* 163, 726–738.
- Isaaks, E.H., Shrivastava, R.M., 1989. *Applied Geostatistics*. Oxford Univ. Press, New York.
- Kachanoski, R.G., 1993. Estimating soil loss from changes in Cs^{137} . *Canadian Journal of Soil Science* 73 (4), 629–632.
- Kachanoski, R.G., DeJong, E., 1984. Predicting the temporal relationship between soil cesium-137 and erosion rate. *Journal of Environmental Quality* 13 (2), 301–304.
- Krezoski, J.R., 1989. Sediment reworking and transport in eastern Lake Superior: in situ rare earth element tracer studies. *Journal of Great Lakes Research* 15 (1), 26–33.

- Land, M., Ohlander, B., Ingri, J., Thunberg, J., 1999. Solid speciation and fractionation of rare earth elements in a spodosol profile from northern Sweden as revealed by sequential extraction. *Chemical Geology* 160 (1–2), 121–138.
- Mahler, B.J., Bennett, P.C., Zimmerman, M., 1998. Lanthanide-labeled clay: a new method for tracing sediment transport in karst. *Ground Water* 36 (5), 835–843.
- Markert, B., 1987. The pattern of distribution of lanthanide elements in soils and plants. *Phytochemistry* 26 (12), 3167–3170.
- Matisoff, G., Ketterer, M.E., Wilson, C.G., Layman, R., Whiting, P.J., 2001. Transport of rare earth element-tagged soil particles in response to thunderstorm runoff. *Environmental Science and Technology* 35, 3356–3362.
- Matisoff, G., Bonniwell, E.C., Whiting, P.J., 2002. Soil erosion and sediment sources in an Ohio watershed using beryllium-7, cesium-137, and lead-210. *Journal of Environmental Quality* 31 (1), 54–61.
- Olmes, I., Pink, F.X., 1994. New particle-labeling technique for use in biological and physical sediment transport studies. *Environmental Science Technology* 28, 1487–1490.
- Olson, K.R., Gennadiev, A.N., Jones, R.L., Chernyanskii, S., 2002. Erosion patterns on cultivated and reforested hillslopes in Moscow Region, Russia. *Soil Science Society of America Journal* 66, 193–201.
- Plante, A.F., Duke, M.J.M., McGill, W.B., 1999. A tracer sphere detectable by neutron activation for soil aggregation and translocation studies. *Soil Science Society of America Journal* 63, 1284–1290.
- Ritchie, J.C., McHenry, J.R., 1990. Application of radioactive fallout Cesium-137 for measuring soil erosion and sediment accumulation rates and patterns: a review. *Journal of Environmental Quality* 19, 215–233.
- SAS Institute, 1990. SAS/STAT Users Guide. Version 6.12. SAS Institute, Gary, NC.
- Sutherland, R.A., 1994a. Spatial variability of ¹³⁷Cs and the influence of sampling on estimates of sediment redistribution. *Catena* 21, 57–71.
- Sutherland, R.A., 1994b. Caesium-137 soil sampling and inventory variability in reference locations: a literature survey. *Hydrological Processes* 10 (1), 43–53.
- Tian, J.L., Zhou, P.H., Liu, P.L., 1994. REE tracer method for studies on soil erosion. *International Journal of Sediment Research* 9, 39–46.
- Toth, S.J., Alderfer, R.B., 1960. A procedure for tagging water-stable soil aggregates with Co-60. *Soil Science* 89, 36–37.
- USDA, 1980. Soil and Water Resource Conservation Act. USDA, Washington, DC.
- USEPA, 1995. Test Methods for Evaluating Solid Waste-SW846, Update III, 3rd ed. US Government Printing Office, Washington, DC.
- Ventura, E., Nearing, M.A., Norton, L.D., 2001. Developing a magnetic tracer to study soil erosion. *Catena* 43 (4), 277–291.
- Wallbrink, P.J., Murray, A.S., 1993. Distribution and variability of Be-7 in soils under different surface cover conditions and its potential for describing soil redistribution processes. *Water Resources Research* 32 (2), 467–476.
- Wallbrink, P.J., Murray, A.S., 1996. Distribution and variability of Be-7 in soils under different surface cover conditions and its potential for describing soil redistribution processes. *Water Resources Research* 32 (2), 467–476.
- Wallbrink, P.J., Olley, J.M., Murray, A.S., 1994. Measuring soil movement using Cs-137 implications of reference site variability. Variability in stream erosion and sediment transport. IAHS Publication 224, 95–103.
- Wheatcroft, R.A., 1991. Conservative tracer study of horizontal sediment mixing rates in a bathyal basin, California borderland. *Journal of Marine Research* 49, 565–588.
- Wheatcroft, R.A., Olmez, I., Pink, F.X., 1994. Particle bioturbation in Massachusetts Bay: preliminary results using a new deliberate tracer technique. *Journal of Marine Research* 52, 1129–1150.
- Whiting, P.J., Bonniwell, E.C., Matisoff, G., 2001. Depth and areal extent of sheet and rill erosion based on radionuclides in soils and suspended sediment. *Geology* 29 (12), 1131–1134.
- Wooldridge, D.D., 1965. Tracing soil particle movement with Fe-59. *Soil Science Society of America Proceedings* 29, 469–472.
- Wyttenbach, A., Furrer, V., Schileppi, P., Tobler, L., 1998. Rare earth elements in soil and in soil-grown plants. *Plant and Soil* 199, 267–273.

- Young, R.A., Holt, R.F., 1968. Tracing soil movement with fluorescent glass particles. *Soil Science Society of America Journal* 32, 600–602.
- Zhang, X.C., Fredrich, J.M., Nearing, M.A., Norton, L.D., 2001. Potential use of rare earth oxides as tracers for soil erosion and aggregation studies. *Soil Science Society of America Journal* 65, 1508–1515.
- Zhang, X.C., Nearing, M.A., Polyakov, V.O., Friedrich, J.M., 2003. Using rare earth oxide tracers for studying soil erosion dynamics. *Soil Science Society of America Journal* 67, 279–288.